

Revision of the Cenozoic Seismic Velocity Structure of the CIROS-1 Drillhole, Antarctica, and Implications for Further Drilling Off Cape Roberts

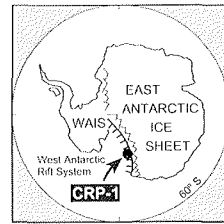
C.J. BÜCKER¹, S.A. HENRYS² & T. WONIK¹

¹GGA, Joint Geoscientific Research Institute, Hannover - Germany

²Institute of Geological and Nuclear Sciences, Lower Hutt - New Zealand

Received 15 July 1998; accepted in revised form 9 October 1998

Abstract - The CIROS-1 drillhole, which in 1986 reached a depth of 700 m below the seafloor, is still the only deep hole that can provide information on the velocity structure of the upper crust in McMurdo Sound and the Ross Sea, Antarctica. A careful review and quality control of the downhole logging data of CIROS-1 resulted in a new porosity depth function that is consistent with porosity data from the MSSTS-1 and CRP-1 drillholes. Using existing porosity-velocity equations, it was possible for the first time to obtain reliable velocity information for the upper 700 m of strata off the Victoria Land coast. The calculated synthetic seismograms, based on downhole velocity and density data, fit very well with the existing seismic lines IT90A-71, PD90-12, and NBP9601-89. The quality of the correlation confirms that the average velocity of the top 700 m of strata is about 2 000-2 300 m/s, and not 2 800-3 000 m/s, as was previously assumed. In consequence, these distinctly lower velocities result in shallower depths for the seismic unconformities V3/V4 and V4/V5 and thus may have important implications for further drilling off Cape Roberts.



INTRODUCTION

One of the main objectives of the Cape Roberts Project (CRP) is to establish a Cenozoic stratigraphy that can be correlated with the large amount of seismic reflection data available from the western side of McMurdo Sound and the Ross Sea. Correlation of geological and geophysical logs with seismic data requires knowledge of P-wave velocities provided by sonic logs and measurements on core samples. However, on account of the premature termination of the CRP-1 drillhole in October 1997 at final depth of 147 metres below sea floor (mbsf) (Cape Roberts Science Team, 1998), the CIROS-1 hole, drilled in 1986 (Barrett, 1989), is still the only deep hole that can provide information on the velocity structure of the upper crust in this region. CIROS-1 is located in McMurdo Sound, about 120 km south of the CRP-1 (Fig. 1). The CRP-1 and CIROS-1 drillholes, as well as MSSTS-1 (Barrett, 1986), are situated on the southwestern margin of the Victoria Land Basin, the westernmost of four north-south trending basins formed by extension of the Ross Sea region [for a general overview of the regional geology and seismic stratigraphy see Cooper & Davey (1987), Anderson & Bartek (1992), Barrett et al. (1995), and Bartek et al. (1995)]. The younger strata in these basins have been drilled by the Deep Sea Drilling Project (DSDP) (Hayes et al., 1975) in the central and eastern Ross Sea. The MSSTS-1 and CIROS-1 holes were drilled in the Victoria Land Basin (Barrett, 1986, 1989) down to 227 and 702 mbsf, respectively. Both holes were drilled from fast ice using a land rotary rig. Core recovery was 98% for CIROS-1 and 56% for MSSTS-1. A limited downhole logging program was conducted only in CIROS-1.

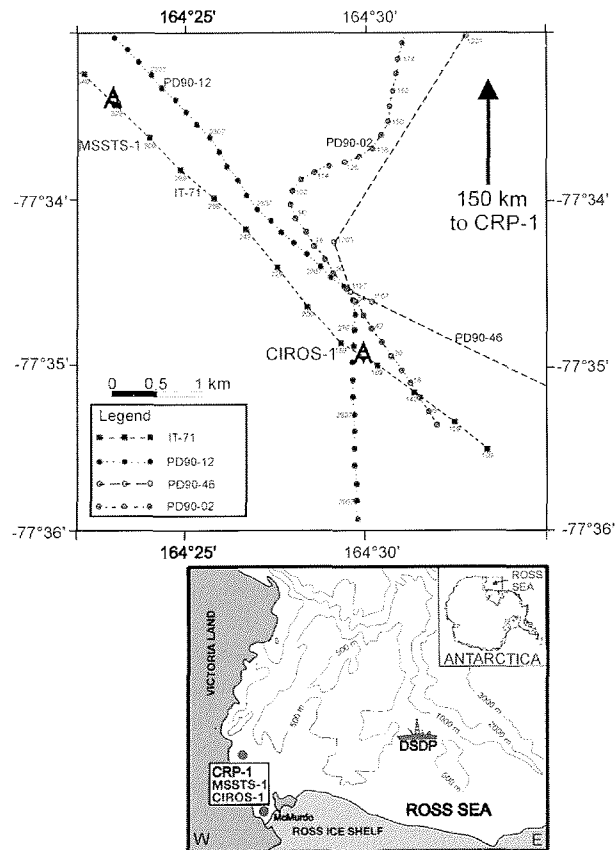


Fig. 1 - Locations of the MSSTS-1, CIROS-1, and CRP-1 drillholes off the western coast of the Victoria Land Basin and detailed map of seismic profiles at MSSTS-1 and CIROS-1. The Italian seismic line IT90A-71 passes directly through the MSSTS-1 and CIROS-1 sites. The Polar Duke lines (PD90) cross 500 m north of the CIROS-1 drilling site. For a detailed location map of CRP-1, see Barrett & Ricci (this volume).

These offshore drilling projects have been carried out to sample strata and to obtain a record of the waxing and waning of the ice sheet in the past. CRP-1, CIROS-1 and MSSTS-1 are the only drillholes on the continental shelf of West Antarctica that provide detailed information on sediment velocities. Interpretation of extensive seismic data (over 40 000 line-km) has relied on correlation with these wells in order to establish a stratigraphy for the western Ross Sea. General seismic sequences have been defined for the Ross Sea by Hinz & Block (1984), for the Eastern Basin and Central Trough by Anderson & Bartek (1992), for the Victoria Land Basin by Cooper & Davey (1987) and Brancolini et al. (1995), and for McMurdo Sound by Bartek et al. (1995). For a discussion of the correlation of the different stratigraphic nomenclatures, see Henrys et al. (this volume).

In the CIROS-1 drillhole, the upper part of the drilled sequence, *i.e.* above the unconformity at 366 mbsf, consists of diamictites, mudstones, sandstones and some conglomerate of early Oligocene to earliest Miocene age (31–22 Ma; Barrett, 1989). The lower part is deep-water mudstone with turbidite sand and conglomerate and some diamictite, ranging from early Oligocene to middle Eocene in age (Bartek et al., 1995). This unconformity is identified on seismic records as the regional V3/V4 boundary of Cooper & Davey (1987). This boundary is equivalent to RSU 6 of Brancolini et al. (1995) and Q/R of Bartek et al. (1995) and Barrett et al. (1995). Seismic correlations between the CIROS-1 and MSSTS-1 drillholes are given by Brancolini et al. (1995), Bartek et al. (1995) and Brancolini & Coren (1997). Reflection times were converted to depths using a weighted average of the stacking velocities in the vicinity the drill sites (Brancolini et al., 1995). In ANTOSTRAT (1995) the strata velocities have been calculated by averaging many velocity analyses from multichannel seismic data in the area of CIROS-1 and MSSTS-1. Reflection coefficients have been obtained empirically from sand/silt/clay concentrations (De Santis et al., 1995; Brancolini & Coren, 1997). Bartek et al. (1995) used the CIROS-1 downhole porosity data to obtain velocity information. Seismic refraction sonobuoy studies in the Ross Sea were undertaken by Cochrane et al. (1993) and by Cooper et al. (1987) for the western Ross Sea and McMurdo Sound.

Calculated synthetic seismograms in these studies differ significantly from those obtained by the previous authors, but, at the same time, provide useful correlation with observed data. In view of the importance of the seismic correlations at the CIROS-1 site to basin-wide stratigraphy in the Ross Sea, we felt it was timely to carefully review the geophysical log data at CIROS-1.

In this paper we present a revised porosity depth function for CIROS-1. This is used to calculate synthetic seismograms, which are then compared with all available seismic data. The results are important for tying the seismic data to CIROS-1. Seismic profiles used for this study were acquired during the 1989/90 Italian OGS-Explora cruise (MCS multichannel survey, line IT90A-71; Brancolini et al., 1995) and the single-channel seismic data during the 1990 Polar Duke cruise (SCS lines PD90-02, PD90-12, PD90-46; Anderson & Bartek, 1992, Fig. 1).

MCS line IT90A-71 passes NE–SW directly across the drill sites CIROS-1 and MSSTS-1, whereas the PD90 lines pass about some hundred metres from the drill sites (Fig. 1).

DOWNHOLE LOGGING DATA AND MEASUREMENTS ON CORES

In the DSDP drillholes in the Ross Sea (Leg 28), core recovery was poor and neither downhole nor core logging was undertaken; hence we have no direct information on seismic velocities. The first information on seismic velocities for the Victoria Land Basin offshore was obtained by measurements on cores from the MSSTS-1 drillhole (Collen & Frogatt, 1986; Frogatt, 1986). Analysis of porosity, density, and velocity measurements on the well lithified core samples below 18 mbsf suggests that a kilometre or more of overlying sediments have been removed by erosion, resulting in unusually high density and velocity, and low porosity values for this depth of sediment. In addition, we believe there might be a bias towards higher density and velocity values due to poor core recovery and poor core quality in the upper 70 m. Density ranges from 1.8 to 2.7 g/cm³, corresponding to high sonic velocities (2–5 km/s). Core porosities vary between 5 and 45% with an average of 27%.

Geophysical logs of hole diameter (caliper), natural radioactivity (GR), bulk density (RHOB), and neutron porosity (NPHI) were obtained in the CIROS-1 drillhole (White, 1989). In general, the logs show a close correlation with lithology (Fig. 2). Sandstone beds having lower natural radioactivity, higher density and lower porosity than mudstone. The diamictites, and especially the conglomerates, are characterised by the highest density and lowest porosity values. Gamma ray values are also low in these sections. The conglomerates clearly cause significant variations in the physical parameters between 320 and 366 mbsf, and at 620 mbsf. The sequence between 320 and 366 mbsf consists of alternating layers of diamictite and conglomerate, the main unconformity probably being at 342 m or 366 m. This unconformity is interpreted to be the seismic sequence boundary V3/V4 (see also Bartek et al., 1995). The average neutron-porosity of the entire column is 13% (gray curve in Fig. 2; data from White, 1989). In contrast to this low average neutron-porosity, porosity measurements on cores from the CRP-1 drillhole (Cape Roberts Science Team, 1998) show an average value of 39% in the depth range between 20 and 147 mbsf. Unfortunately, no sonic log was carried out in CIROS-1. Bearing in mind that strata has been eroded from the sequences drilled by the CIROS and MSSTS, an average porosity of 13% for the CIROS site appears anomalously low in comparison with the average values of 27% and 39% for the MSSTS and CRP-1 sites (Niessen et al., this volume).

CALCULATION OF POROSITY

How can we explain the discrepancy between the relatively low porosity values obtained for CIROS-1

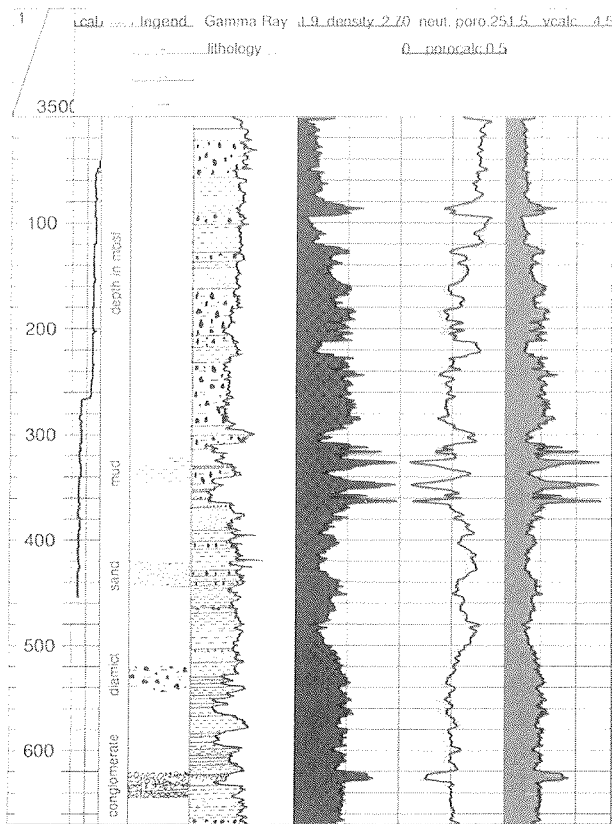


Fig. 2 - Downhole geophysical logs measured in CIROS-1 (White, 1989) together with a simplified lithology (Barrett, 1989) showing mudstone, sandstone, diamictite, and conglomerate. Depth is given in metres below seafloor (mbsf). From left to right: (1) drillhole diameter (caliper) in mm; (2) lithology legend; (3) simplified lithology and natural radioactivity (gamma ray, not calibrated to API); (4) density from 1.9 to 2.7 g/cm², measured by gamma-ray attenuation; (5) light gray curve, measured neutron porosity (neut. poro.) from 0% to 25%, black curve shows the calculated porosity (porocalc) from 0% to 50%; and the (6) calculated velocity (vealc) from 1.5 to 4.5 km/s (see text for explanation).

compared with measurements made on cores from MSSTS-1 and recent samples obtained from CRP-1? White (1989) described the calibration procedure of the neutron-porosity probe using measurements on miniplugs taken from the CIROS core. The disadvantage of miniplugs is the biased nature of the sampling procedure, *i.e.* only intact cores were used for sampling. This gives preference to lower porosities (and higher densities). Secondly, it seems that the given plug porosities are calculated as weight percent (water-filled pores) rather than the usual volume percent porosities; hence, porosity is underestimated. As an alternative method, we have derived a new porosity (Φ) curve, calculated from the downhole density ρ , the matrix density ρ_{ma} (mainly quartz and calcite with an average density of 2.67 g/cm³) and the fluid density ρ_{fl} (salt water 1.02 g/cm³) using

$$\Phi = \frac{\rho_{ma} - \rho}{\rho_{ma} - \rho_{fl}}$$

These new, calculated volume percent porosities are almost twice as large as previously published porosities. The new downhole porosity log is given in figure 2 (second column from right, black curve). However, the

average value of the new calculated porosities is 28%, close to the average value obtained from the MSSTS cores, confirming our doubts about the original neutron-porosity calibration procedure. In short, we believe the neutron-porosity probe should be recalibrated. Despite differing by a factor of two, the “old” neutron-porosity curve and the “new”, calculated density-porosity curve show excellent correlation. The differences between the old neutron-porosities and the new ones can be clearly seen in the frequency distribution (Fig. 3).

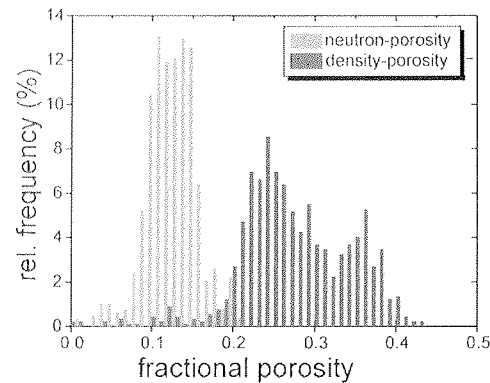


Fig. 3 - Frequency distribution of fractional porosities in CIROS-1. Gray: downhole measured neutron porosities. Black: calculated density-derived porosities (see text for formula). The density-derived porosities are twice as large as the neutron porosities. We believe the neutron porosities are too low and have to be recalibrated.

CALCULATION OF VELOCITY

A velocity curve can be derived from the newly calculated porosity curve. Relationships between velocity and porosity of sediments are given in the recent literature, and several procedures for deriving velocity from porosity are described. A comprehensive review of the existing equations is given by Erickson & Jarrard (in press). The relationships between porosity and velocity as given by the different authors are shown graphically in figure 4. Wyllie et al. (1956) introduced an empirical equation for

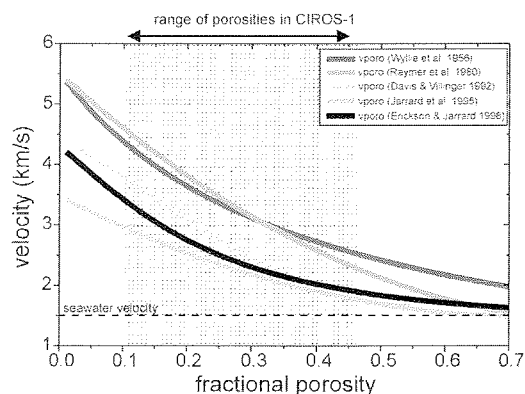


Fig. 4 - Curves of velocity-porosity equations from different authors. The range of porosities for the CIROS-1 drillhole is shaded. Velocity data for the CIROS-1 hole were calculated using the density-derived porosity values and the Jarrard et al. (1995) equation (see text for details).

the relationship between p-wave velocity V_p and porosity Φ for low-porosity sandstones using the matrix velocity V_{ma} and the fluid velocity V_f to calculate compressional wave velocities:

$$1/V_p = \Phi/V_f + (1 - \Phi)/V_{ma}$$

This empirical equation results in relatively high velocity values over the entire range of porosities between 0% and 70% (Fig. 4). The Wyllie equation, also known as the time-average relation, has been successfully used by log analysts in the petroleum industry. The Raymer et al. (1980) equation, which takes all types of porosity into account, contains a squared term for porosity and is different from the Wyllie equation, especially for high porosity sediments (see Fig. 4). Davies & Villinger (1992) combined several equations for high porosity and low porosity, resulting in a cubic relationship between velocity and porosity. They state that their equation is valid over a porosity range of 10–57%. The most recent equations are presented by Jarrard et al. (1995) and Erickson & Jarrard (in press). These equations take into account log-based porosities and velocities from the Cascadia accretionary prism and other ODP (Ocean Drilling Program) holes. According to Jarrard et al. (1995), a second-order polynomial regression shows a good fit to the p-wave velocity data (V_p) for the undeformed sediments at Cascadia:

$$V_p = 3.48 - 5.42 \Phi + 3.69 \Phi^2$$

The Erickson & Jarrard (in press) relation takes into account many factors that affect the velocity. The differences from the earlier Jarrard et al. (1995) model are mainly due to the shale content and consolidation history, and can be seen particularly well in the low porosity range. Both these papers give a validity range for porosities of 20–70%. In this porosity range the differences for shale-free marine siliciclastic sediments are lower than 5% in the corresponding velocity range. For the following investigations, the downhole velocity for the CIROS-1 drillhole was calculated using the Jarrard et al. (1995) equation (lowermost, medium-grey curve in Fig. 4), and is shown in figure 2 (right column).

The frequency distribution of velocity as a function of the lithology (Fig. 5) shows a roughly trimodal structure, and an overall average velocity of 2.25 km/s can be inferred. The mudstones and some of the diamictites display low velocities at 2.0 km/s, whereas the conglomerates have the highest velocities, *i.e.* around 2.8 km/s and a few above 3.0 km/s. The sandstones and some of the diamictites are characterised by intermediate velocities at about 2.4 km/s. Only the conglomerates show velocities higher than 2.6 km/s.

The velocity-porosity relations of both Jarrard et al. (1995) and Erickson & Jarrard (in press) show excellent correlation with the data from the CRP-1 core (Cape Roberts Science Team, 1998) in the high porosity range above 25% (Fig. 6). This confirms the two models and justifies the calculation of velocities from porosities based on their models for the CIROS-1 drillhole. The observed

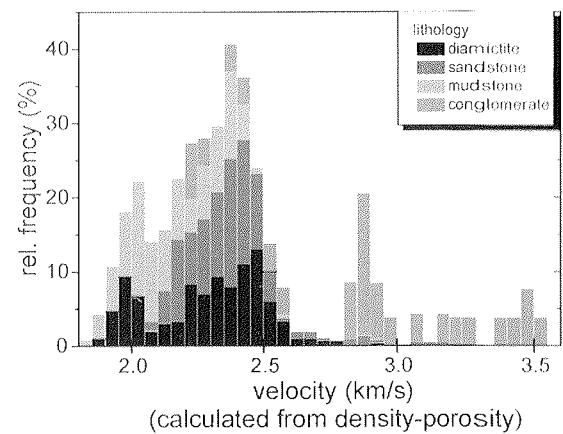


Fig. 5 - Frequency distribution of calculated velocities for CIROS-1 showing lithologies. The conglomerates show the highest velocities and the mudstones the lowest (lithologies from Barrett, 1989).

deviation from their equations at low porosities is due to the variation in lithology and the different mechanical properties of the limestones that were found in CRP-1. The physical properties of the CRP-1 core are discussed in detail in Niessen et al. (this volume) and Jarrard et al. (this volume).

GENERATION OF SYNTHETIC SEISMOGRAMS AND CORRELATION WITH SEISMIC LINES

Reliable downhole density and velocity data, as well as seismic impedances $z = \rho v$, and reflection coefficients $R = (z_2 - z_1)/(z_2 + z_1)$, permitted synthetic seismograms to be calculated.

Synthetic seismograms were generated using a reflectivity algorithm (Kennett, 1981). This method

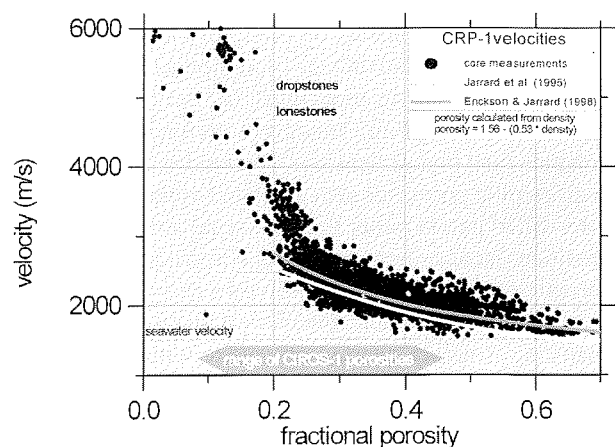


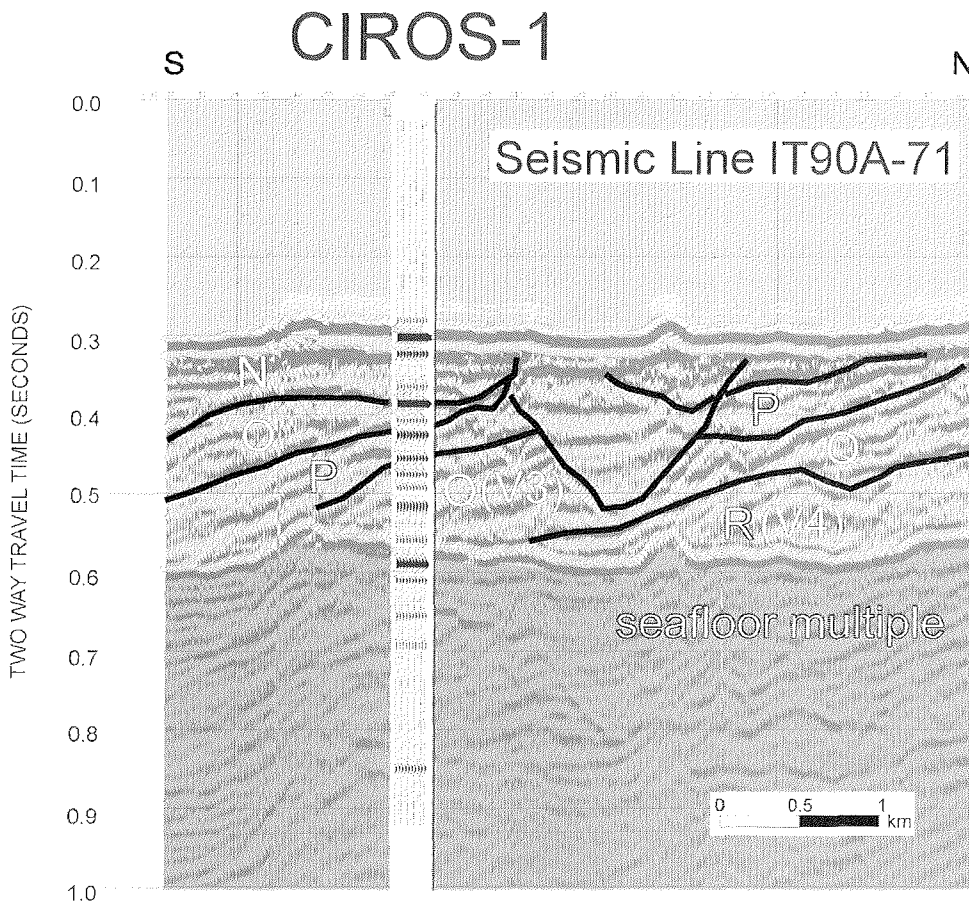
Fig. 6 - Comparison of the curves for the Jarrard et al. (1995) and Erickson & Jarrard (in press) velocity-porosity equations with the porosities measured on cores from the CRP-1 drillhole (Cape Roberts Science Team, 1998). Note the good correlation in the porosity range above 0.25. The limestones dominate the lower porosity range; however, limestones were not included in the porosity-velocity equations mentioned above.

accounts for all normally incident waves and their multiples, seafloor multiples are not included. Input is in terms of P-wave velocity, density, porosity, attenuation, and depth or thickness of horizontal layers. In all cases presented here, attenuation is assumed to be infinite. No attenuation measurements were made on core samples and, unless Q (seismic wave attenuation quality factor) is low, velocity dispersion effects are assumed to be small. Velocity, density and porosity values for the different layers, apart from the sediments immediately below the seafloor, were derived from well logs and measurements on core samples. The properties of the seafloor were determined by trial-and-error matching of the observed and calculated water bottom reflections. The synthetic traces were subjected to the same processing sequence as the observed single-channel seismic data (*i.e.* same filter and gains) and displayed with identical plotting parameters. Single-channel data (SCS) from PD90 and near-trace multichannel data (MCS) from IT90A-71 (CIROS-1) and NBP9601 (CRP-1) were used. These data sets include a minimum amount of processing to preserve both true amplitude and relative trace-to-trace amplitudes, *i.e.* no deconvolution or FK filtering, or trace averaging was applied. On lines IT90A-71, PD90-12, and NBP9601, the ten traces close to the drillholes were substituted for the synthetic traces (Figs. 7, 8, & 9).

The seismic traces were not migrated. The effect of migrating data is to steepen dipping structures, but near-surface, gently dipping events retain their shallow dip. Accurate migration requires detailed velocity information, which is not available for single-channel data. However, migration of near-trace data from IT90A-71, using velocity information from multichannel processing, steepened the slopes of glacial channels, but data in the vicinity of the wells remained unaffected.

SYNTHETIC SEISMOGRAMS AND CORRELATION WITH SEISMIC LINES AT CIROS-1

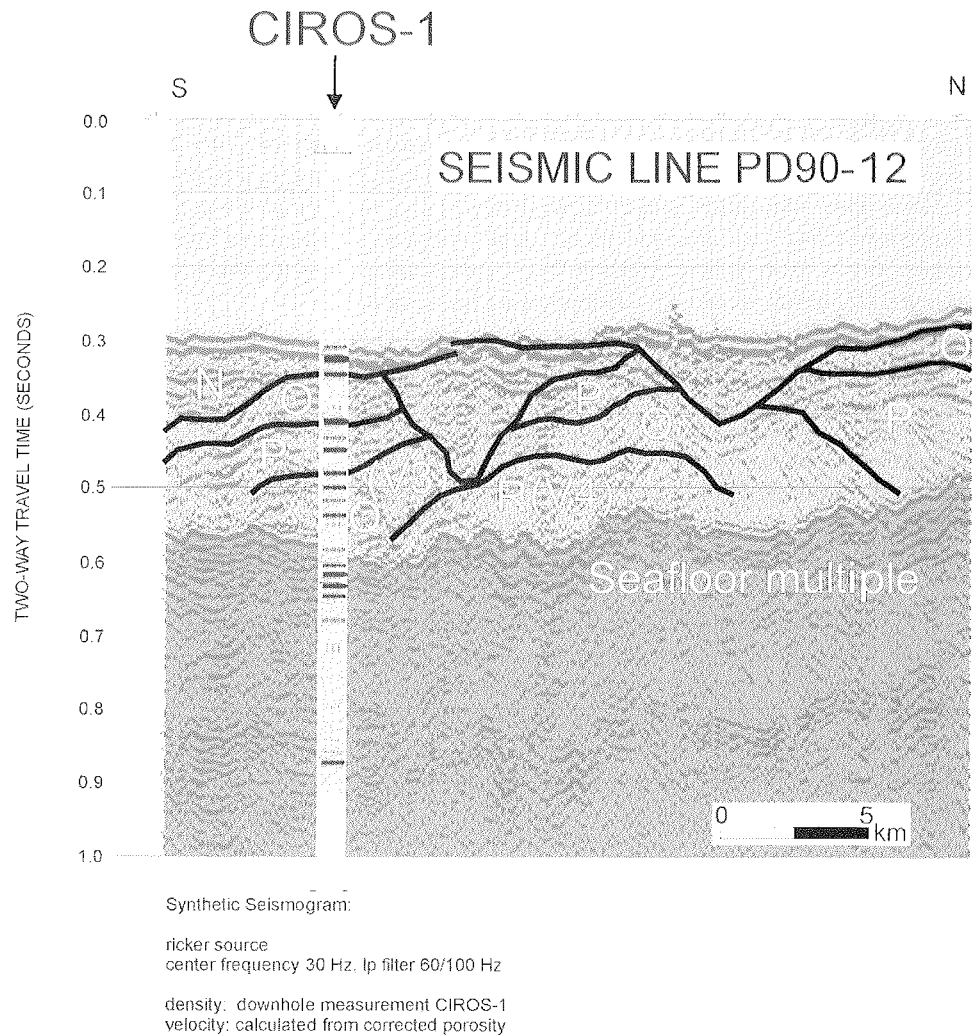
Figure 7 shows an expanded view of seismic line IT90A-71 and the synthetic CIROS-1 seismogram. The seismic reflectors show excellent correlation with all the reflections in the synthetic traces. This is remarkable because the IT90A-71 line is a low frequency line (10–20 Hz). Bartek et al. (1995) grouped velocities into 20 distinct layers (average 2 800 m/s) for their synthetic seismogram calculations and compared the results with seismic line PD90-12 (location see Fig. 1). The main difference in our calculations is that a finer detail of the velocity and density logs was used, resulting in a more



Synthetic seismogram:
 low frequency ricker source
 center frequency 10 Hz, lp filter 35/80 Hz
 density: measured in CIROS-1
 velocity: calculated from density-porosity

Fig. 7 - Seismic line IT90A-71 (Brancolini et al., 1995) and the calculated synthetic seismogram for the CIROS-1 drillhole. The unconformity (V3/V4) is visible at 580 ms in the synthetic CIROS-1 seismogram just below the seafloor multiple, and appears to lie on the continuation of an unconformity visible in the seismic section as a southward dipping reflector beneath the glacial channel. This means that for the first time the V3/V4-boundary can be traced into a drillhole log, thus providing reliable information on its depth. All reflectors in the seismogram above the seafloor multiple can be clearly correlated with reflectors in the synthetic trace.

Fig. 8 - Seismic line PD90-12 (Anderson & Bartek, 1992) and the synthetic seismogram for the CIROS-1 drillhole, both at higher frequency than those in figure 7. Although this seismic profile is about 200 m from CIROS-1 (see Fig. 1), most of the reflectors can be correlated with reflections in the synthetic trace. In contrast to figure 7, three reflectors are visible just below the seafloor multiple in the synthetic CIROS-1 seismogram, the lowest one of which is probably the 366 mbsf unconformity (V3/V4, and Q/R boundary between stratigraphic units Q and R from Fig. 3 of Bartek et al. (1995)). This lowest reflector appears to correlate with the southward-dipping reflector below the glacial channel.



detailed synthetic seismogram. The average velocity in the CIROS-1 well from the revised velocity log is now 2 250 m/s. This has the effect of shifting reflectors to greater two-way travel times (TWT) (shallower depths) in the seismogram time sections. For example, the reflection between stratigraphic units Q and R at 578 ms TWT in Bartek et al. (1995; Fig. 3) is now at 630 ms TWT, a difference of more than 50 ms TWT. This reflection between units Q and R corresponds to the V3/V4 boundary, which is inferred to be at 366 mbsf in figure 2, and is also a distinct reflector in the synthetic seismograms.

Unfortunately, the seafloor multiple reflections are a major limitation to identifying primary reflections at times greater than 580 ms TWT. Nevertheless, a reflection in the synthetic traces just below the multiple at 580 ms TWT can be seen to be the continuation of the southward-dipping reflector below the glacial channel structure north of the CIROS-1 drillhole. This reflection below 580 ms TWT can be correlated with the three velocity peaks between 325 and 366 mbsf in figure 2 and is therefore attributed to the V3/V4 boundary. This means that for the first time a reflection interpreted to be the V3/V4 boundary, can be reliably incorporated in drilling results, and one can be reasonably confident about its depth.

An expanded view of seismic line PD90-12 and its correlation with the synthetic CIROS-1 seismogram is

given in figure 8. The PD90 data are medium frequency (30–50 Hz), thus showing a more detailed reflection structure than the IT90A-71 line. The synthetic seismograms were processed in the same manner as the seismic lines, also resulting in more detail than that of the IT90A-71 synthetic traces. In figure 8 there is also a very good match between almost all the seismic reflectors and the synthetic seismogram. Again, the reflection due to the main unconformity in CIROS-1 occurs just below the seafloor multiple, and appears to be a continuation of the southward-dipping reflector more clearly visible in figure 7.

SYNTHETIC SEISMOGRAMS AND CORRELATION WITH SEISMIC LINES AT CRP-1

The synthetic seismogram for the CRP-1 site is superimposed on part of seismic line NBP9601-89 in figure 9 (for the location of seismic lines NBP96 see Henrys et al., this volume). The synthetic traces are based on density and velocity measurements on the core from CRP-1 (Niessen et al., this volume). The average velocity of the sediments in the CRP-1 drillhole is 2 000 m/s (Fig. 6). The limestones, which show high velocities,

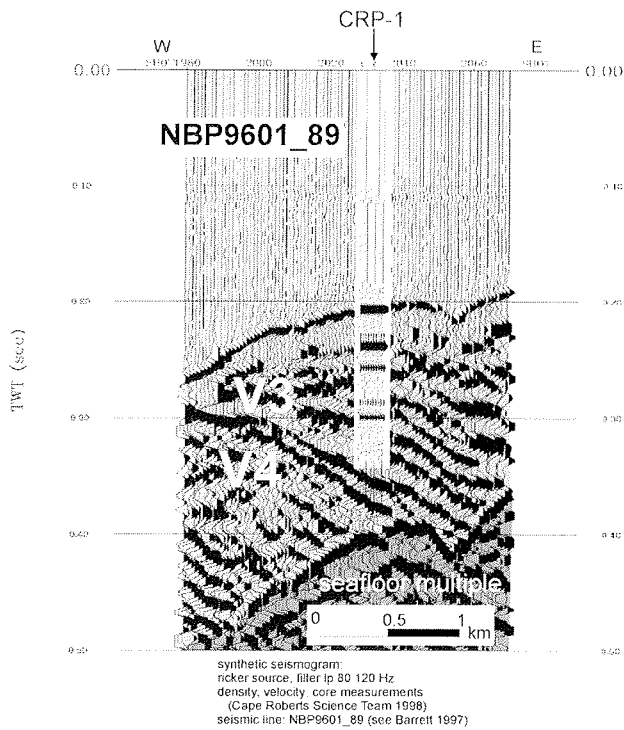


Fig. 9 - Seismic line NBP9601_89 (Barrett, 1997) and synthetic seismogram for the CRP-1 drillhole. The upper constraint of the V3/V4 boundary is indicated (Bartek et al., this volume), the CRP-1 drillhole missed this boundary by a few metres. Water depth is 150 m. The seismic data from the CRP-1 site consist of near-traces extracted from a 22-channel MCS data set acquired as part of USAP Nathaniel B. Palmer cruise 9601.

appear to have little influence on the average velocity. The low average velocity is consistent with the CIROS-1 results and gives a total drilling depth of 345 ms TWT for the CRP-1 hole, which must terminate just a few metres above the estimated position of the V3/V4 boundary (Cape Roberts Science Team, 1998).

The reflection at the base of the Quaternary section at 44 mbsf, due to a drop in velocity and an increase in porosity, can be seen to occur in the seismic section and synthetic seismogram at 240 ms. In the Miocene section below, three major reflections can be traced in the synthetic traces. Henrys et al. (1994) subdivided the seismic stratigraphic units V2 and V3 into at least six seismic sequences on the basis of the single-channel seismic line NBP96 in McMurdo Sound. However, most of these sequences pinch out on the eastern flank of Roberts Ridge and exact correlation of Miocene and older units with CRP-1 remains uncertain (see Henrys et al., this volume).

DISCUSSION AND CONCLUSIONS

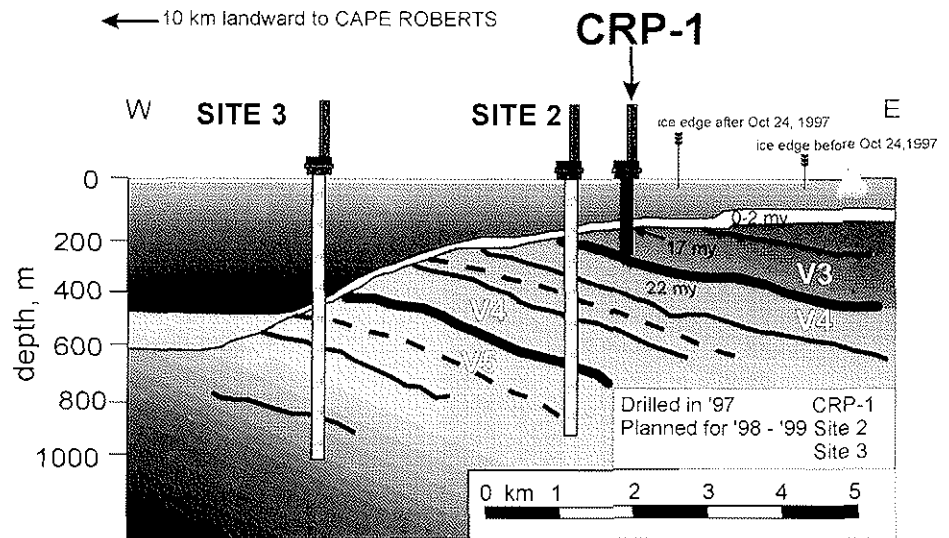
Currently, the large amount of available seismic data can be interpreted only by correlating it with CIROS-1 and MSSTS-1 logs as well as with DSDP 273 results in order to establish a Cenozoic stratigraphy for the western Ross Sea. However, new porosity measurements from cores from CRP-1 have highlighted a discrepancy in the neutron porosity log of CIROS-1 (White, 1989). A new porosity

curve based on the original density logs now provides data that is reliable and consistent with measurements on core samples. In addition, synthetic seismograms that use the velocity profile based on the new porosity data match the observed seismic data very closely. Furthermore, these measurements indicate lower values of P-wave velocity than previously assumed for McMurdo Sound and the Victoria Land Basin. This may also have some implications for the entire Ross Sea. As to our knowledge, seismic depth sections given so far are based on velocity measurements on cores, downhole porosity measurements, calculation of stacking velocities (Davy & Alder, 1989; Brancolini et al., 1995), seismic refraction sonobuoy studies (Cooper et al., 1987), or indirect methods for determination of reflectors. The velocities measured on MSSTS-1 (Frogatt, 1986) and CIROS-1 (Davy & Alder, 1989) cores appear to be far too high. It is now clear that these high core velocities do not reflect the *in-situ* situation. They may have several causes. Whole-core segments, free of fractures and with no clasts in the sediment, were chosen for the measurements (Frogatt, 1986). This fact, together with the effects of the cores being allowed to dry out (the measurements were made some time after coring), may have biased the velocities towards higher values. Also the procedure of calculating stacking velocities during seismic processing tends to give higher velocities, particularly in areas with dipping reflectors. According to the seismic refraction sonobuoy studies by Cooper et al. (1987, p. 109), they gave a velocity range of 2.9 – 4.1 km/s for seismic unit V3.

The newly calculated downhole porosities for the CIROS-1 drillhole are in good agreement with the MSSTS-1 and CRP-1 values, taking into account the thickness of the eroded part of the sequence at the CIROS-1 site. It has been shown, that the Jarrard et al. (1995) and the Erickson & Jarrard (in press) velocity-porosity equations are also well suited for the strata drilled in McMurdo Sound, thus justifying calculation of velocity from porosity. Bearing in mind that the geological situations at the CIROS-1 and CRP sites are not identical (part of the sequence at CIROS-1 having been removed by erosion), the results for the calculated porosities and velocities at the CIROS 1 site are conclusive and comparable to the values measured on cores from CRP 1. This indicates that the CRP-1 core measurements have produced reliable results.

The best correlation between the synthetic seismogram and a seismic section through the CIROS-1 site is displayed by the Italian IT90A-71 line. This low frequency (and thus low resolution) line passes directly through the drill site and at an angle of 45° to the Victoria Land Basin structure, giving a good basis for a comparison. All reflectors from the seismogram above the seafloor multiple can be traced into the synthetic seismogram. The PD90 lines 02, 12 and 46 cross about 500 m north of the CIROS-1 drilling location, complicating correlation with CIROS-1. Although the medium-frequency line PD90-12 does not show as good a correlation with the synthetic traces as the line IT90A-71 does (Fig. 7), most of the reflectors can also be matched in this seismic section (Fig. 8). Because of the distance and the sharp bend just north of the CIROS site, line PD90-46 is not suitable for comparison with CIROS-1.

Fig. 10 - Drilling sites off Cape Roberts together with a simplified seismic line drawing (adapted from Barrett et al., 1998). CRP-1 was drilled in October 1997 down to 147 mbsf. Sites 2 and 3 are planned for the 1998 and 1999 seasons, respectively. This cross-section through the Cape Roberts sequence is based on seismic data from NBP9601-89 assuming a velocity of 2 200 m/s for the upper 700 m. Drillsites from which the entire sequence can be cored with two 700 m deep drill holes are also indicated.



SUMMARY AND IMPLICATIONS FOR FURTHER DRILLING OFF CAPE ROBERTS

Significantly improved velocity data for the upper 700 m of Cenozoic strata off the Victoria Land coast has been derived by re-evaluating and re-calculating the CIROS-1 logging data. The calculated synthetic seismograms, based on the downhole velocity and density data, fit very well with the low-frequency seismic line IT90A-71, which passes directly through the drillhole location. The higher-frequency, and thus the higher-resolution seismic line PD90-12, which passes some distance from the drillhole location, also shows a good correlation with the synthetic seismograms. These correlations represent further confirmation of an average velocity of about 2 000–2 300 m/s for the top 700 m of strata, instead of 2 800–3 000 m/s previously derived from the stacking velocities (Davy & Alder, 1989; Brancolini et al., 1995) and poorly calibrated porosity data from the CIROS-1 drillhole. Lower average velocities mean that the strata, and more important, unconformities inferred to correspond to V3/V4 and V4/V5, are shallower than previously thought. Figure 10 presents a cross-section through the Cape Roberts sequence based on seismic data from NBP9601-89 assuming a velocity of 2 200 m/s for the upper 700 m. Drillsites from which the entire sequence can be cored with two 700 m deep drill holes are also indicated.

ACKNOWLEDGEMENTS

Seismic data from NBP96-01 was provided courtesy of L.R. Bartek and B.P. Luyendyk. IT90A-71 data was provided by Giuliano Brancolini (*Osservatorio Geofisico Sperimentale*, Trieste, Italy). This paper benefited much from discussions with Richard Jarrard. Frank Niessen made all the CRP-1 core measurements and kindly made them available to us. Constant encouragement and support from Franz Tessensohn is gratefully acknowledged. We also thank Helga Wiederhold, Christian Reichert and Fred Davey for their reviews of the manuscript.

CRP is an international project. The German part is funded by Alfred-Wegener-Institute for Polar and Marine Research, DFG (German Science Foundation) and the BGR (Federal Institute for Geosciences and Natural Resources, Hannover). New Zealand participation is funded by PGSF under contract to the Foundation for Research Science and Technology.

REFERENCES

- Anderson J.B. & Bartek L.B., 1992. Cenozoic Glacial History of the Ross Sea Revealed by Intermediate Resolution Seismic Reflection Data Combined with Drill Site Information. In: Kennett J.P. & Warnke D.A. (eds.), *The Antarctic Paleoenvironment: a Perspective on Global Change*, part one, *AGU Antarctic Research Series*, **56**, Washington DC, 231-263.
- ANTOSTRAT Project, 1995. Seismic Stratigraphic Atlas of the Ross Sea, Antarctica. In: Cooper A.K., Barker P.F. & Brancolini G. (eds.), *Geology and Seismic Stratigraphy of the Antarctic Margin*, *AGU Antarctic Research Series*, **68**, Washington DC.
- Barrett P.J. (ed), 1986. Antarctic Cenozoic history from the MSSTS-1 drillhole, McMurdo Sound. *DSIR Bulletin*, **237**.
- Barrett P.J. (ed), 1989. Antarctic Cenozoic history from the CIROS-1 drillhole, McMurdo Sound. *DSIR Bulletin*, **245**.
- Barrett P.J., 1997. Cape Roberts Science Plan. *Antarctic Data Series*, **20**, Victoria University of Wellington, 59 p.
- Barrett P.J., Henrys S.A., Bartek L.R., Brancolini G., Busetti M., Davey F.J., Hannah M.J. & Pyne A.R., 1995. Geology of the Margin of the Victoria Land Basin off Cape Roberts, Southwest Ross Sea. In: Cooper A.K., Barker P.F. & Brancolini G. (eds.), *AGU Antarctic Research Series*, **68**, Washington DC, 183-207.
- Bartek L.R., Henrys S.A., Anderson J.B. & Barrett P.J., 1995. Seismic Stratigraphy of McMurdo Sound, Antarctica: Implications for Glacially Influenced Early Cenozoic Eustatic Change? *Marine Geology*, **130**.
- Brancolini G., Cooper A.K. & Coren F., 1995. Seismic Facies and Glacial History in the Western Ross Sea (Antarctica). In: Cooper A.K., Barker P.F. & Brancolini G. (eds.), *AGU Antarctic Research Series*, **68**, Washington DC, 209-233.
- Brancolini G. & Coren F., 1997. Seismic Correlation between CIROS-1 and MSSTS-1 Drill Holes. Ross Sea, Antarctica. In: Davies F. et al. (eds.), *Glaciated Continental Margins. An Atlas of Acoustic Images*, Chapman & Hall, London, 238-241.
- Cape Roberts Science Team, 1998. Initial Report on CRP-1, Cape Roberts Project, Antarctica. *Terra Antarctica*, **5**(1), 187 p.
- Cochrane G.R., Cooper A.K., Childs J.R., Hart P.E. & Brancolini G., 1993. Preliminary Results of a 1989 Seismic Refraction Survey in the Ross Sea, Antarctica. *Geol. Jb.* **E47**, 313-333.

- Collen J.D. & Frogatt P.C., 1986. Depth of burial and hydrocarbon source rock potential. In: Barrett P.J. (ed.), *Antarctic Cenozoic history from the MSSTS-1 drillhole, McMurdo Sound, DSIR Bulletin*, **237**.
- Cooper A.K., Barker P.F., Webb P.N. & Brancolini G. (eds.), 1994. The Antarctic Continental Margin: Geophysical and Geological Stratigraphic Records of Cenozoic Glaciation, Paleoenvironments and Sea-level Change. ANTOSTRAT-Symposium, Siena. *Terra Antarctica*, **1**(2), 480 p.
- Cooper A.K. & Davey F.J., 1987. The Antarctic continental margin: geology and geophysics of the western Ross Sea. *Circumpacific Council on Economic and Mineral Resources Earth Science Series*, **5B**, Houston.
- Cooper A.K., Davey F.J. & Cochrane G.R., 1987. Structure of Extensionally Rifted Crust Beneath the Western Ross Sea and Iselin Bank, Antarctica, from Sonobuoy Seismic Data. In: Cooper A.K. & Davey F.J. (eds.), *The Antarctic continental margin: geology and geophysics of the western Ross Sea, Circumpacific Council for Energy and Mineral Resources Earth Science Series*, **5B**, Houston.
- Davies E. & Villinger H., 1992. Tectonic and thermal structure of the Middle Valley sedimented rift, northern Juan de Fuca Ridge. In: Davies E., Mottl M.J. et al. (eds.), *Proc. ODP, Init. Repts.*, **139**, 9-41.
- Davy B.W. & Alder G., 1989. Seismic reflection surveys. In: Barrett P. (ed.), *Antarctic Cenozoic history from the CIROS-1 drillhole, McMurdo Sound, DSIR Bulletin*, **245**.
- De Santis L., De Cillia C. & Marchetti A., 1995. Seismic Stratigraphic Atlas of the Ross Sea, Antarctica: MSSTS-1 and CIROS-1. In: Cooper A.K., Barker P.F. & Brancolini G. (eds.), *Geology and Seismic Stratigraphy of the Antarctic Margin, AGU Antarctic Research Series*, **68**, Washington DC.
- Erickson S.N. & Jarrard R.D., in press. Velocity-Porosity Relationships for Siliclastic Sediments and Rocks. *J. Geophys. Res.*
- Frogatt P.C., 1986. Seismic velocities. In: Barrett P.J. (ed.), *Antarctic Cenozoic history from the MSSTS-1 drillhole, McMurdo Sound, DSIR Bulletin*, **237**.
- Hayes D.E., Frakes L.A. et al., 1975. *Init. Rep. DSDP*, **28**, 1017 p.
- Henry S.A., Bartek L.R., Anderson J.B. & Barrett P.J., 1994. Seismic Stratigraphy in McMurdo Sound: Correlation of High Resolution Data Sets. *Terra Antarctica*, **1**, 373-374.
- Hinz K. & Block M., 1984. Results of geophysical investigations in the Weddell Sea and in the Ross Sea, Antarctica. In: *Proceedings 11th World Petrol. Congress*, London, Wiley, New York, 279-291.
- Jarrard R.D., MacKay M.E., Westbrook G.K. & Screation E.J., 1995. Log-based porosity of ODP sites on the Cascadia accretionary prism. In: Carson B., Westbrook G.K. et al. (eds.), *Proc. ODP, Sci. Results*, **146**, 313-335.
- Kennett B.L.N., 1981. Elastic wave propagation in stratified media. In: *Advances in applied mechanics*, New York, Academic press, Inc, **21**, 79-167.
- Raymer L., Hunt E.R. & Gardner J.S., 1980. An improved sonic transit time-to-porosity transform. *Trans. SPWLA 21st Ann. Logging Symp.*, P1-P13.
- White P., 1989. Downhole Logging. In: Barrett P. (ed.), *Antarctic Cenozoic history from the CIROS-1 drillhole, McMurdo Sound, DSIR Bulletin*, **245**.
- Wyllie M.R.J., Gregory A.R. & Gardner L.W., 1956. Elastic wave velocities in heterogeneous and porous media. *Geophysics*, **21**, 41-70.